MEDFARM: Jurnal Farmasi dan Kesehatan, Vol. 14, No. 2, 2025, Page 408-422
e-ISSN : 2715-9957
p-ISSN: 2354-8487

Computational Analysis of Biflavonoid Derivatives through Molecular Docking on ALK Kinase Receptor as Potential Inhibitors of A549 Cell Proliferation

Feri Kanti Rahayu[1*], Arinda Nur Cahyani[2], Syaiful Prayogi[3], Dossy Susan Anggraeni[4], Putri Aulia Zahra[5], Azzahra Rhisma Ernanda[6], Indah Fajar Falupi[7], Dila Rahma[8]

[1,2,7)]Prodi S1 Farmasi, STIKes Ibnu Sina Ajibarang, Jalan Raya Ajibarang-Tegal Km.01, Ajibarang, Jawa Tengah 53163, Indonesia
[3,4,5,6)]Prodi S1 Farmasi, Fakultas Sains dan Teknologi, Universitas Peradaban, Jalan Raya KM 3 Paguyangan, Paguyangan-Brebes, Jawa Tengah 52776, Indonesia
[8)]Prodi D3 Analis Farmasi dan Makanan, STIKes Ibnu Sina Ajibarang, Jalan Raya Ajibarang-Tegal Km.01, Ajibarang, Jawa Tengah 53163, Indonesia

e-mail:
ferikantirahayu@gmail.com

ABSTRACT

Globally, lung cancer remains among the foremost causes of death associated with malignancy. In the Indonesian population, it is positioned as the third most common cancer after cervical and breast cancers, and non-small-cell lung carcinoma (NSCLC) constitutes the predominant form, accounting for about 85–88% of reported cases. Anaplastic lymphoma kinase (ALK) is a key molecular target in NSCLC, contributing significantly to carcinogenesis. However, resistance to current ALK-targeted therapies poses a major challenge. To address this, new drug discovery efforts are urgently needed. While drug development is typically time-consuming and costly, Computer-Aided Drug Design (CADD) offers an efficient strategy at the early stages. Biflavonoid derivatives have shown anticancer potential but are limited by poor solubility and low activity, warranting further optimization. This study explores structural modifications of biflavonoid derivatives to identify potential ALK inhibitors. The results demonstrate that the modified compounds (Compounds A and B) exhibit binding affinities comparable to the reference drug, Entrectinib. Furthermore, ADMET predictions indicate favorable oral absorption, adequate systemic distribution, and a relatively safe toxicity profile, supporting the potential of these compounds as novel anticancer candidates.

Keywords: ALK, NSCLC, proliferation

Introduction

Cancer persists as one of the principal contributors to global mortality and continues to impose a heavy public health burden. Data from the World Cancer Research Fund indicate that in 2022, around 19.9 million new cases were recorded worldwide, with 10.3 million in men and 9.7 million in women. Among various cancer types, lung cancer ranks as the second most prevalent malignancy, following breast

cancer, with an estimated 2.48 million cases and 1.82 million deaths reported globally (WCRF, 2022) (Ferlay et al., 2021).

Lung cancer contributes to approximately 8.8% of new cancer diagnoses in Indonesia, making it the third leading cancer following breast and cervical cancers (Globocan, 2020), Notably, over **70% of lung cancer patients** in Indonesia are in their **productive age group (<59 years)**, exhibiting a **lower quality of life** compared with patients diagnosed with other cancer types (Dewi et al., 2021). As reported by the Indonesian Ministry of Health (2018), In Indonesia, lung cancer ranks as the second major contributor to cancer mortality, responsible for approximately 15.9% of reported cancer deaths, with men being disproportionately affected (Kementerian Kesehatan Republik Indonesia, 2018).

Lung cancer, when evaluated based on histopathological characteristics, falls into two major types SCLC and NSCLC. Notably, NSCLC represents the predominant form, comprising nearly 85–88% of all reported cases. The A549 human lung adenocarcinoma cell line, derived from hypotriploid alveolar basal epithelial cells, serves as a well-established in vitro model for NSCLC research (Korrodi-Gregório et al., 2016). This cell line is commonly employed to evaluate the antiproliferative and cytotoxic potential of various chemical and natural compounds.

At the molecular level, ALK has been identified as a key oncogenic driver in a subset of NSCLC cases (Kifle et al., 2021). Aberrant activation of the ALK gene through amplification, mutation, or its overexpression is known to promote both tumor initiation and advancement in multiple cancers, including lung cancer, inflammatory myofibroblastic tumors, and neuroblastoma (Della Corte et al., 2018). Even with FDA-approved ALK TKIs such as crizotinib, ceritinib, entrectinib, and alectinib the development of drug resistance greatly limits their long-term clinical benefit (Lin et al., 2017). Consequently, the development of novel ALK-targeted agents remains an important focus in NSCLC therapy (Kifle et al., 2021).

Standard therapeutic approaches for lung cancer, such as surgical resection, radiotherapy, chemotherapy, and targeted treatment, are often accompanied by severe adverse effects, limited therapeutic efficacy, and high rates of drug resistance. These limitations not only affect treatment outcomes but also have a profound impact on patients' psychological well-being and recovery (Morrissey et al., 2016). Therefore, there is an urgent need to discover new anticancer agents that are safer, more selective, and pharmacologically efficient, particularly compounds targeting ALK in NSCLC.

In this context, biflavonoids, a class of bioactive secondary metabolites, have attracted increasing attention as promising anticancer candidates. These compounds are widely distributed in the Selaginellaceae family, with approximately 80 biflavonoids reported in the *Selaginella* genus (Zou et al., 2021). Natural biflavonoids are known to possess a broad spectrum of biological activities, including notable antioxidant, anti-inflammatory, and anticancer properties. The anticancer potential of these compounds involves mechanisms like apoptosis induction, angiogenesis inhibition, and metastasis suppression (Jung et al., 2017). Notably, fifteen biflavonoid derivatives isolated from *Selaginella doederleinii* were shown to significantly inhibit

the proliferation of NSCLC A549 cells with varying IC_{50} values (Zou et al., 2021)(Muema et al., 2022).

Despite their promising bioactivity, natural biflavonoids suffer from poor solubility in both aqueous and lipid media, leading to low oral bioavailability and limited clinical applicability (Ren et al., 2023). To overcome these challenges, structural modification and computational drug design approaches have been proposed to enhance their pharmacokinetic profiles and safety characteristics. Computational modeling enables the rational design of new therapeutic agents with improved potency, selectivity, and stability, while minimizing toxicity and development costs. Such in silico approaches can significantly accelerate drug discovery and reduce experimental trial-and-error, providing a cost-effective and efficient strategy for developing novel ALK-targeted anti-NSCLC agents (Siswandono, 2016).

Methodology

This research utilized an in silico strategy through molecular docking simulations. The target protein was the three-dimensional crystal structure of ALK kinase (PDB ID: 5FTO), obtained from the RCSB Protein Data Bank. The evaluated ligands were biflavonoid derivatives that had undergone specific structural modifications.

Hardware used in this study consisted of a laptop with the following specifications: The system is powered by an AMD Ryzen™ 7 6800H mobile processor featuring 8 cores and 16 threads, with a 20 MB cache and boost speeds reaching 4.7 GHz. It is equipped with 32 GB of DDR5-4800 SO-DIMM memory (2 × 16 GB) and a 512 GB PCIe® 4.0 NVMe™ M.2 solid-state drive for storage. Graphics performance is supported by an NVIDIA® GeForce RTX™ 3050 laptop GPU. The device includes a 15.6-inch OLED Full HD display (1920 × 1080) in a 16:9 aspect ratio, rated at 250 nits with an anti-glare surface. The operating system installed is Windows 11 64-bit.

Software employed in this research included: **iGEMDock** (for molecular docking analysis); **Discovery Studio Visualizer** (for protein-ligand interaction visualization); **Marvin Sketch** (for ligand structure design and modification); and **ADMETSAR** (web-based application for physicochemical, pharmacokinetic (ADME), drug-likeness, and toxicity prediction).

Structure Modifications

The **Topliss scheme** was employed as a guideline for compound modification. This approach involves the introduction of substituent groups with distinct lipophilic, electronic, and steric features are introduced at predetermined sites on the core scaffold of the lead molecule. Such modifications are predicted to enhance the biological activity of the compounds compared to the parent structure (Lazzarotto et al., 2005).

Preparation of Target Macromolecular Structure

The three-dimensional structure of ALK kinase was obtained from the Protein Data Bank (PDB). The structure was prepared by removing **H_2O molecules** and separating the reference ligand using **Discovery Studio Visualizer (DSV)**. The

prepared structure was then saved in ***.pdb** format and used as the target macromolecule for the subsequent *molecular docking* process (Huey et al., 2012).

Preparation of Test Ligand Structures

The test ligands used in this study were modified compounds designed and modeled using **Marvin Sketch**. The ligand structures were then saved in the appropriate format for the molecular docking process.

Docking Method Validation

Docking validation was performed using **iGEMDock**. The validation criteria were based on the **RMSD (Root Mean Square Deviation)** values, defined as follows: **RMSD ≤ 1 Å** : excellent conformation, closely resembling the native structure; **1 Å < RMSD ≤ 2 Å** : good conformation, approximating the native structure; **2 Å < RMSD ≤ 3 Å** indicates a conformation with clear deviations or structural inaccuracies, while RMSD values exceeding **3 Å** reflect a poorly reproduced conformation.

Docking of Test Ligands

Docking of the test ligands was performed using parameter settings identical to those employed during the validation process.

Result and Discussion

Lead Compound Structure and Modified Sites

The lead compound utilized in this study was a **biflavonoid derivative**. Structural modifications were performed at specific substitution sites (**R1 to R5**) to design novel derivatives with potentially enhanced biological activity. The structure of the biflavonoid lead compound with the designated modification sites is presented in **Figure 1**, while the modified derivatives are illustrated in **Figure 2**.

Structural modifications were carried out by introducing **–OH** at position **R4**, **$-N(CH_3)_2$** at position **R5**, and **$-CH_3$** at position **R6** (Figures 1 and 2). These modifications were expected to enhance the biological activity of the compounds. The incorporation of **$-CH_3$** and **$-N(CH_3)_2$** groups was predicted to increase the **lipophilicity**, thereby potentially improving the pharmacological activity. This is consistent with the statement of Siswandono (2016), which emphasized that optimal activity can be achieved by introducing substituents capable of enhancing the lipophilic properties of a compound (Siswandono & Soekardjo, 2017).

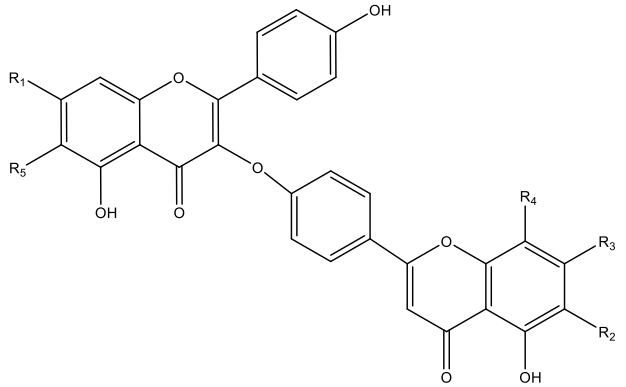

Figure 1. Lead compound

MEDFARM: Jurnal Farmasi dan Kesehatan, Vol. 14, No. 2, 2025, Page 408-422
e-ISSN : 2715-9957
p-ISSN: 2354-8487

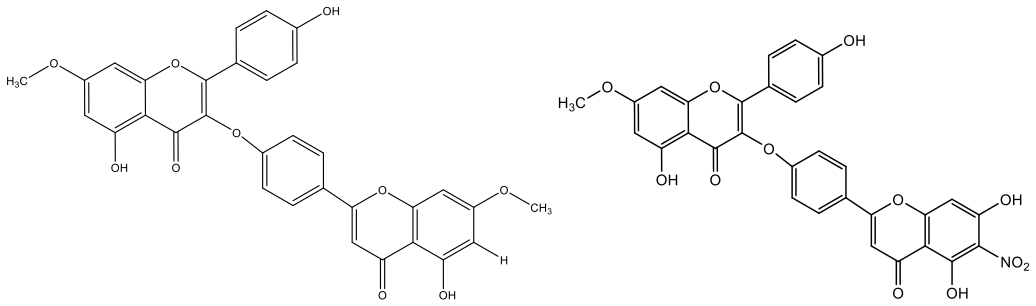

A B

Figure 2. Modified structure

The **co-crystal structure of the target protein** is presented in **Figure 3**. The preparation of **ALK Kinase** (PDB ID: 5FTO) (Jawarkar et al., 2022) was performed by removing **H_2O molecules** and separating the native ligand using **Discovery Studio Visualizer (DSV)**. The processed structure was then saved in ***.pdb** format. This protein target was selected based on its high-quality resolution data, with a resolution of **2.22 Å**, which meets the requirement of < 2.5 Å. The structure was determined by **X-ray diffraction** method. Furthermore, the protein contains a native/reference ligand, **Entrectinib**, which was employed as a comparator in the docking validation process.

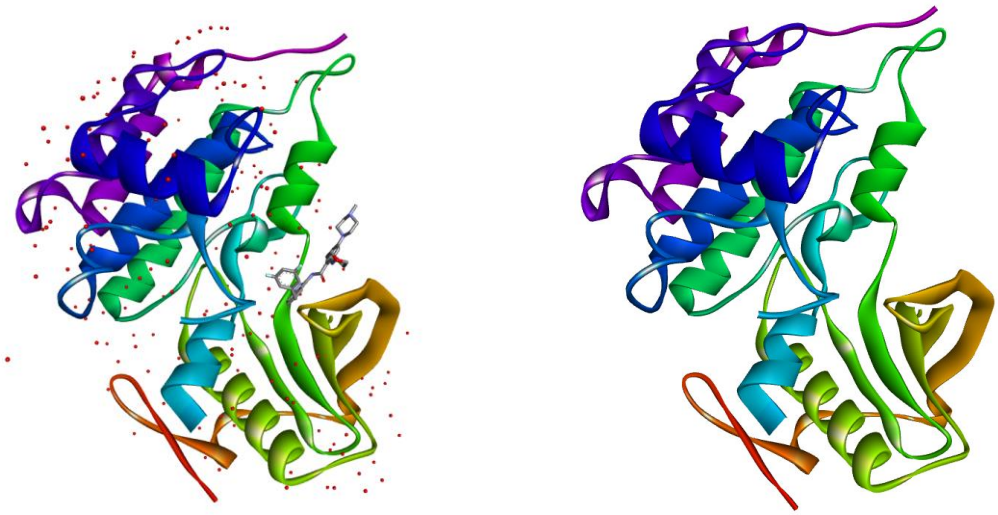

A B

Figure 3. **Target protein and reference ligand.** Crystal structure of ALK Kinase before preparation (A) and after preparation (B). The preparation was carried out by removing H_2O molecules and separating the native ligand (Entrectinib) using Discovery Studio Visualizer (DSV).

The *re-docking* results of the reference ligand with **ALK Kinase** are presented in **Figure 4** and **Table 2**. A docking method is considered valid if it meets the following criteria: (1) the **Root Mean Square Deviation (RMSD)** between the re-docked pose and the crystallographic structure is ≤ 2 Å; (2) the amino acid residue interaction profile is consistent; and (3) the intermolecular interactions between ligand and protein are preserved (Sari et al., 2020). Based on the *re-docking* results, the RMSD

MEDFARM: Jurnal Farmasi dan Kesehatan, Vol. 14, No. 2, 2025, Page 408-422
e-ISSN : 2715-9957
p-ISSN: 2354-8487

value obtained was 1.9 **Å (≤ 2 Å)**, indicating that the docking method applied in this study is valid.

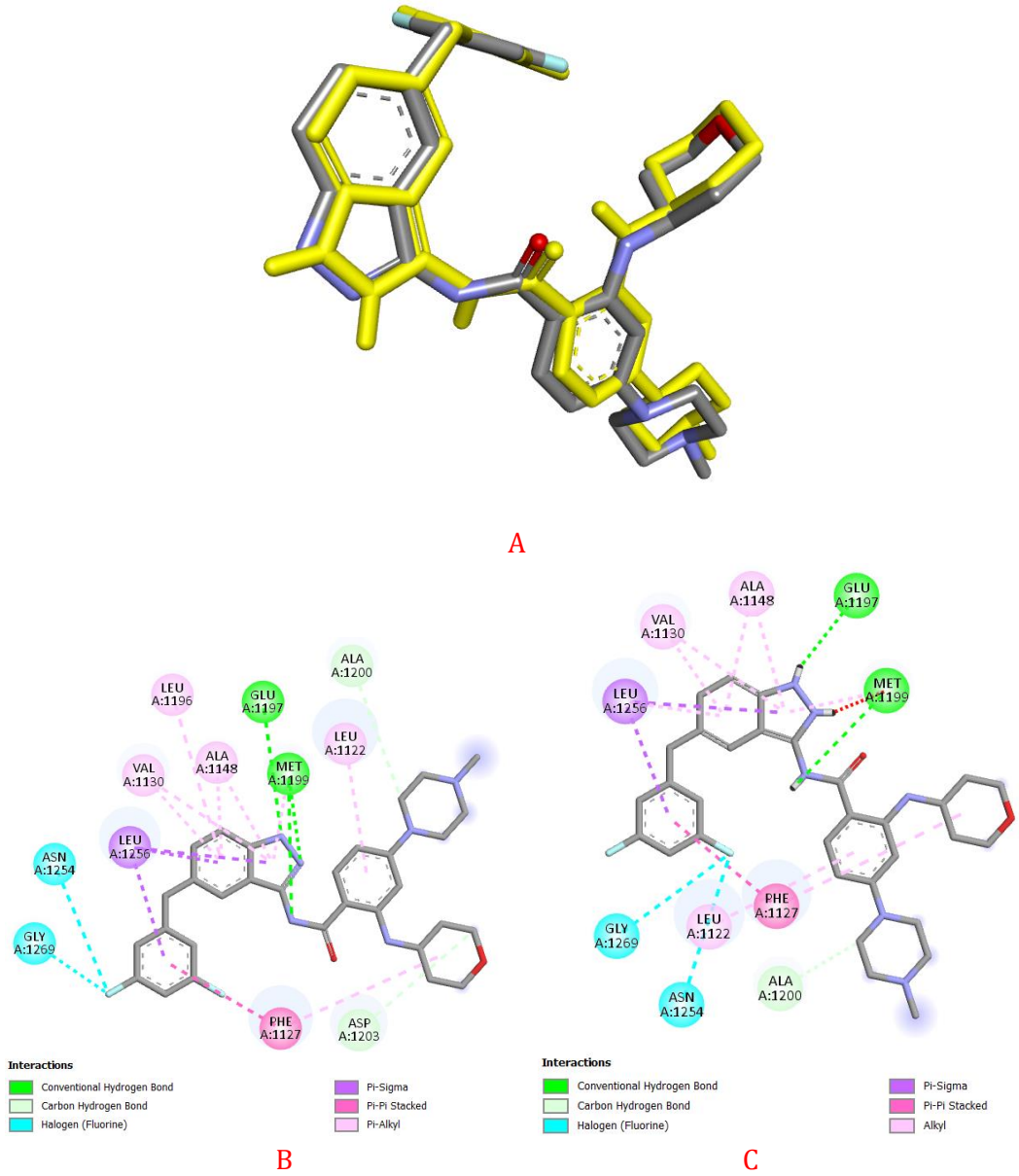

Figure 4. **Docking Validation of ALK Kinase.** Superimposition of the reference ligand Entrectinib in the co-crystal structure (metallic) and in the re-docked pose (yellow) (A); interaction profile of co-crystallized Entrectinib with amino acid residues (B); and interaction profile of re-docked Entrectinib (C).

Docking Results of Test Compounds against the Target Protein

The newly designed compounds A and B (figure 2) were docked into the target protein using the same parameters applied in the docking validation, as shown in Figure 5 and Table 1. The results revealed that the test ligands exhibited binding energies comparable to the reference ligand. The interactions observed between the

test ligands and the protein involved multiple types of interactions, primarily hydrophobic and hydrogen bonding. Analysis indicated that the amino acid residues **VAL A: 1130**; **LEU A:1256**; **PHE A: 1127**; **ALA A:1148**; **and GLU A:1197** represent critical active site residues responsible for ligand/inhibitor binding (Table 2). This is supported by the observation that these residues consistently appeared in the interactions of the co-crystal, re-docking, and test ligand docking results, predominantly forming hydrogen bonds. Hydrophobic interactions are considered the dominant factor contributing to the stability of the protein–ligand complex, while hydrogen bonds also play a stabilizing role, albeit to a lesser extent. Furthermore, hydrophobic forces are essential in driving the association of non-polar drug moieties with the non-polar regions of the biological receptor. Non-polar drug molecules can induce the formation of *quasi-crystalline* (icebergs) structures in surrounding water molecules through hydrogen bonding. Therefore, hydrophobic interactions are key determinants in maintaining the stability of protein–ligand complexes.

Table 1**. Docking Parameters of Novel Compounds A and B against ALK**

Ligan	Binding Energy (ccal/moL)
Entrectinib	-11,0
A	-8,8
B	-8,3

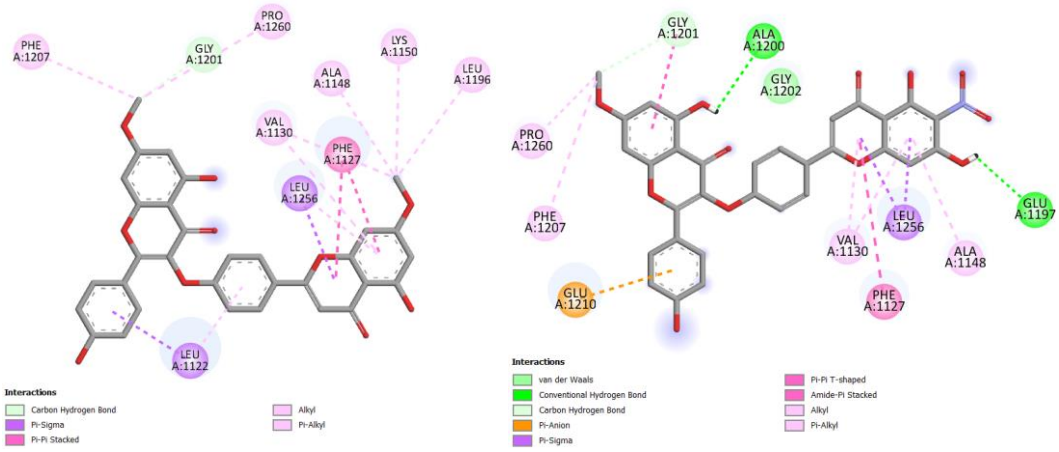

A B

Figure 5. **Docking Visualization Compounds to ALK Kinase.** interaction profile of Compound A (A) and interaction profile of Compound B (B).

Table 2. **Interaction profile**

Ligan	Binding Type			
	Hydrogen	Hidrofobic	Electrostatic	Other
Entrectinib	GLU A:1197; MET A:1199; ALA A:1200	**Alkyl:** VAL A: 1130; ALA A:1148; LEU A:1256 **Pi-Alkyl**: LEU A:1122; PHE A: 1127; ALA A:1148; VAL A:1130; MET A:1199 **Pi-Pi Stacked:** PHE A:1127 **Pi-Sigma:** LEU A:1256	-	ASN A:1254; GLY A:1269
A	GLY A:1201	**Alkyl:** PRO A:1260; VAL A:1130; ALA A:1148; LYS A:1150; LEU A:1196	-	- VAL A: 1130; LEU A:1256; PHE A: 1127;

		Pi-Alkyl: LEU A:1122; LEU A:1256; VAL A:1130; PHE A:1207 **Pi-Sigma:** LEU A:1122; LEU A:1256 **Pi-Pi Stacked:** PHE A:1127		ALA A:1148; and GLU A:1197
B	ALA A:1200; GLU A:1197; GLY A:1201	**Alkyl:** PRO A:1260 **Pi-Alkyl:** VAL A:1130; PHE A:1207; ALA A:1148 **Pi-Sigma:** LEU A:1256 **Pi-Pi Stacked:** GLY A:1201; GLY A:1202 **Pi-Pi T-shaped:** PHE A:1127	**Pi-Anion:** GLU A: 1210	-

ADMET Profile

Pharmacokinetic assessment is essential to determine the in-body behavior of a new drug candidate. In this work, the ADME characteristics of the synthesized derivatives were predicted using the AdmetSAR platform. Each model compound and its parent structure were analyzed to enable direct comparison of their pharmacokinetic performance. The SMILES identifiers were submitted to the system, which subsequently generated the predicted values for all relevant parameters. The absorption profiles of the newly designed molecules are summarized in Table 3.

Table 3. **Absorption Prediction Newly Design Compound**

Compound	HIA* (%)	Caco-2 (cm/sec)**
Ref.	**94.1**	**0.15**
Lead	**89.3**	**0.21**
A	93.5	0.279
B	80	0.03

**Human Intestinal Absorption (HIA): high >70%, moderately 20-70%, poorly 0-20%*
***Colorectal Cell Culture (Caco-2): high (1) low (0)*

Studies indicate that the predicted Caco-2 permeability values of the newly designed compounds fall within the low-permeability range, although compound A demonstrates the most favorable permeability profile among all candidates. In contrast, three other compounds exhibit limited permeability, with compound B showing the lowest value—even lower than the parent compound. This reduced permeability is consistent with the physicochemical characteristics of biflavonoids, which tend to behave as weak bases at physiological pH (5–7), leading to higher ionization and diminished membrane permeation (Dai et al., 2018).

Despite their low Caco-2 permeability, the biflavonoid-derived model compounds show high human intestinal absorption (HIA), with values exceeding 70%. However, compound B displays lower absorption compared with the parent molecule (80%). Caco-2 cells, derived from human colon adenocarcinoma, are widely used as an in vitro model to evaluate oral drug absorption via intestinal epithelial transport. Permeability values <4 nm/sec indicate poor permeability, whereas values >70 nm/sec represent high permeability (Puspita, 2018).

The predicted absorption outcomes are consistent with previously established criteria. (Pires et al., 2015b) stated that compounds with optimal oral absorption typically show HIA values above 80%, reflecting efficient uptake in the small intestine, the principal site of oral drug absorption (Chander et al., 2017).

Table 4. **Distribution Prediction Newly Design Compound**

Compound	BBB*	PPB**
Ref.	**0.305**	**94.8**
Lead	**0.175**	**100**
A	0.276	100
B	0.057	100

**Blood Brain Barrier (BBB) Penetration: High >2,0; Middle 2,0-0,1; Low <0,1*
***Plasma Protein Binding (PPB): Strongly Bound >90% ; Weakly Bound <90%*

Table 4 presents the predicted distribution profiles of the tested compounds. Compound A demonstrates a moderate capacity to cross the blood–brain barrier (BBB), whereas compound B exhibits low permeability, falling below that of the lead compound. All newly designed molecules show strong plasma protein binding (PPB), suggesting that these compounds are likely to be well-distributed within systemic circulation.

Predicted distribution characteristics are primarily assessed through BBB penetration and plasma protein binding parameters. Compounds with BBB values below the 0.1 threshold are generally considered to have limited absorption into the central nervous system (Pardridge, 2012). PPB reflects the proportion of drug bound to plasma proteins, a parameter known to influence pharmacological activity and systemic distribution. Higher PPB values often correlate with more stable plasma retention and optimized distribution profiles (Nusantoro & Fadlan, 2020; Smith et al., 2018). These findings collectively indicate that the new compound models possess favorable distribution potential.

Table 5. **Prediction Newly Design Compound to cytochrome**

Com.	Inhibitor CYP						Substrat CYP					
	1A2	3A4	2B6	2C9	2C19	2D6	1A2	3A4	2B6	2C9	2C19	2D6
Ref	0.13	0.53	0.53	0.72	0.54	0.24	0.65	0.88	0.28	0.52	0.72	0.52
Lead	0.82	0.13	0.58	0.8	0.56	0.16	0.24	0.29	0.19	0.21	0.09	0.09
A	0.7	0.17	0.64	0.81	0.56	0.11	0.24	0.38	0.20	0.23	0.11	0.10
B	0.63	0.1	0.49	0.72	0.29	0.17	0.23	0.28	0.14	0.23	0.08	0.08

0-0.3 : no potential inhibitor/substrat ; 0.31-0.70 : middle potential inhibitor/substrat ; 0.71-1.0 : very potential inhibitor/substrat

Cytochrome P450 (CYP) profiling is essential for predicting metabolic behavior and potential drug–drug interactions. As shown in Table 5, compound A exhibits strong inhibitory potential toward CYP2C9 (0.81), comparable to the lead compound (0.80), indicating a possible risk of interaction with CYP2C9-metabolized drugs such as warfarin and phenytoin (Zanger & Schwab, 2013). Compound B shows moderate inhibition of CYP2C9 (0.72), suggesting a lower but notable interaction risk.

For CYP1A2, the lead compound displays strong inhibition (0.82), whereas compounds A (0.70) and B (0.63) show only moderate inhibition, indicating that structural modification reduces CYP1A2-related interaction risk. Importantly, both compounds A and B demonstrate low inhibitory potential toward CYP3A4 and CYP2D6 (values <0.30), which is favorable given the dominant role of these isoforms in clinical drug metabolism(Fadlan et al., 2022; Lynch & Price, 2007; Zanger & Schwab, 2013).

Regarding substrate potential, neither compound A nor B shows strong affinity for any CYP isoform (>0.71), in contrast to the reference compound, which is predicted to be a strong substrate of CYP3A4 and CYP2C19. Overall, compounds A and B present a more controlled CYP interaction profile, supporting their further development with manageable metabolic and interaction risks, although CYP2C9 inhibition warrants further experimental validation.

Table 6. **Prediction Exretion Newly Design Compound**

Compound	CLp	CLr	T1/2	MRT
Ref.	**0.33**	**0.55**	**0.25**	**0.27**
Lead	0.66	0.67	0.58	0.59
A	0.45	0.66	0.44	0.45
B	0.59	0.65	0.47	0.49

0-0.3 : low ; 0.31-0.70 : medium ; 0.71-1.0 : high

Predicted excretion parameters (Table 6) provide essential insight into the elimination kinetics of the compounds, particularly their urinary and renal clearance potential. Compounds A and B exhibit moderate renal clearance comparable to the reference. Notably, compound B shows plasma clearance comparable to the lead compound and superior to both the reference and compound A. The calculated half-life ($T_1/_2$) and mean residence time (MRT) for both A and B exceed those of the reference, matching the profile of the lead compound. These pharmacokinetic metrics — total body clearance (CLp), renal clearance (CLr), $T_1/_2$, and MRT — are central to defining dosing regimen and drug elimination dynamics. Plasma clearance reflects the volume of plasma cleared of drug per time unit and determines overall exposure, while renal clearance accounts for drug excretion via the kidneys. Half-life indicates the time for plasma concentration to decline by half, guiding dosing interval, and MRT represents the average time a drug remains in the body, independent of dose (JB & KE, 2008; StatPearls, 2024a, 2024b).

Table 7. **Toxicity Prediction**

Compound	Neurotoxicity	DILI	hERG	Nephrotoxicity	Ames mutagenesis	FDAMDD
Ref.	**0.28**	**0.81**	**0.26**	**0.33**	**0.62**	**0.52**
Lead	0.44	0.59	0.38	0.48	0.46	0.22
A	0.27	0.60	0.60	0.37	0.57	0.36
B	0.45	0.72	0.21	0.53	0.61	0.32

0-0.3 : low ; 0.31-0.70 : medium ; 0.71-1.0 : high

Toxicity assessment was conducted for neurotoxicity, drug-induced liver injury (DILI), hERG inhibition, nephrotoxicity, Ames mutagenicity, and FDAMDD, as summarized in Table 7. The predicted toxicity profiles varied among the tested compounds, with Compound A exhibiting an overall more favorable safety profile than Compound B, particularly in terms of neurotoxicity and hERG inhibition. Compound A showed a low-risk neurotoxicity score (0.27), which was lower than that of Compound B (0.45), categorized as moderate risk. Neurotoxicity represents a critical safety concern due to its direct association with adverse effects on the central and peripheral nervous systems, potentially arising from mechanisms such as mitochondrial dysfunction, oxidative stress, neurotransmitter imbalance,

excitotoxicity, blood–brain barrier disruption, and neuroinflammation(Crofton & others, 2022; Serafini & others, 2024). Early identification of neurotoxic liabilities is therefore essential, given their substantial contribution to late-stage drug attrition.

Regarding hepatotoxicity, all tested compounds demonstrated a lower predicted DILI risk compared with the reference drug, although none outperformed the parent compound. Considering that DILI remains one of the leading causes of clinical trial failure and post-marketing drug withdrawal, this parameter continues to represent a critical aspect of drug safety evaluation (Chen et al., 2021; Huang et al., 2020; RJ et al., 2019). In terms of cardiac safety, Compound B displayed the most favorable predicted hERG profile among the candidates; however, Compound A exhibited a slightly lower hERG inhibition score compared with Compound B (0.60 vs. 0.61). Although both compounds fall within the moderate-risk category, this difference remains pharmacologically relevant, as unintended hERG channel inhibition is closely associated with QT interval prolongation, increased risk of Torsades de Pointes, and sudden cardiac death (Kramer & others, 2013; Sanguinetti & Tristani-Firouzi, 2006).

With respect to nephrotoxicity, Compound A showed a risk profile comparable to that of the reference drug, whereas Compound B and the parent compound indicated a higher likelihood of renal toxicity. Drug-induced kidney injury—including impaired glomerular filtration, tubular damage, inflammation, and crystal deposition—frequently contributes to attrition during clinical development (Mody et al., 2020; Perazella & Rosner, 2022; Tejera et al., 2020). In addition, Ames mutagenicity predictions revealed that Compound A exhibited a more favorable profile than the reference drug, while Compound B demonstrated a mutagenic potential comparable to the reference. The Ames test remains the primary assay for early assessment of genetic damage and base-pair mutation risk in drug discovery (Pires et al., 2015a).

All evaluated compounds, including the parent compound, demonstrated improved FDAMDD predictions relative to the reference drug, although none surpassed the parent compound. The FDAMDD metric provides an estimate of the maximum safe daily exposure derived from medium-term clinical data and serves as an important indicator of long-term safety margins (Chen et al., 2021). Overall, the combination of lower neurotoxicity and reduced hERG inhibition risk positions Compound A as the more promising candidate compared with Compound B, thereby supporting its prioritization for further optimization and experimental validation.

Conclusion

Overall, binding energy analysis revealed that the modified compounds displayed slightly lower affinities toward ALK compared with the reference ligand, Entrectinib (−8.3 to −8.8 kcal/mol), while maintaining interaction patterns with key active-site residues similar to those of the reference. Notably, Compound A exhibited not only a favorable binding profile but also improved ADMET characteristics, particularly in terms of toxicity, relative to Entrectinib. These combined structural, energetic, and pharmacokinetic features highlight the potential of Compound A as a

promising lead candidate for further optimization and experimental validation in the development of ALK-targeted anticancer agents.

Declaration of Competing Interest

The authors declare that there are no conflicts of interest related to this work

Acknowledgment

The authors wish to express their gratitude to the Directorate of Research and Community Service (DPPM), Ministry of Higher Education, Science, and Technology of the Republic of Indonesia, for funding this study through the 2025 Basic Research Programme.

Reference

A, B., MV, H., Y, Z., JC, H., & CE, D. (2020). An Update on the Structure of hERG. *Frontiers in Pharmacology*, *10*, 1572. https://doi.org/10.3389/fphar.2019.01572

A, T.-M., JP, B., A, T., RE, T., RF, T., K, C., A, C., K, W., JJ, N., J, M., P, S., A, K., JR, C., D, T., A, L., J, H., S, G., L, C., & PA, E. (2022). Use of the bacterial reverse mutation assay to predict carcinogenicity of N-nitrosamines. *Regulatory Toxicology and Pharmacology*, *135*, 105247. https://doi.org/10.1016/j.yrtph.2022.105247

B, B., S, A., P, C., & others. (2022). Unveiling urinary mutagenicity by the Ames test: applications and limitations. *Mutation Research/Genetic Toxicology and Environmental Mutagenesis*.

Chander, R., Kumar, V., & Singh, A. (2017). Human Intestinal Absorption Prediction: An Overview of Current Computational Approaches. *Current Drug Metabolism*, *18*(7), 608–621. https://doi.org/10.2174/1389200218666170220102449

Chen, B., Luo, H., Chen, W., Huang, Q., Zheng, K., Xu, D., Li, S., Liu, A., Huang, L., Zheng, Y., Lin, X., & Yao, H. (2021). Pharmacokinetics and Tissue Distribution of Delicaflavone. *Frontiers in Pharmacology*, *12*, 1–12.

Crofton, K. M., & others. (2022). Current status and future directions for a neurotoxicity testing framework. *Neurotoxicology*, *92*, 1–13. https://doi.org/10.1016/j.neuro.2022.06.010

Dai, J., Liang, H., Wu, Y., & Wang, X. (2018). Flavonoids and Their In Vivo Metabolites: Absorption, Bioavailability and Biological Activities. *Food & Function*, *9*(7), 3155–3172. https://doi.org/10.1039/C8FO00529E

Della Corte, C. M., Viscardi, G., Di Liello, R., Fasano, M., Martinelli, E., Troiani, T., Ciardiello, F., & Morgillo, F. (2018). Role and targeting of anaplastic lymphoma kinase in cancer. *Molecular Cancer*, *17*(1), 1–9. https://doi.org/10.1186/s12943-018-0776-2

Dewi, A., Thabrany, H., Satrya, A., Puteri, G. C., Fattah, R. A., & Novitasari, D. (2021). Kanker Paru, Kanker Paling Mematikan Di Indonesia: Apa Saja Yang Telah Kita Atasi Dan Apa Yang Kita Bisa Lakukan. In *PKJS-UI* (pp. 1–29). Pusat Kajian Jaminan Sosial Universitas Indonesia (PKJS-UI).

Fadlan, A., Kurniawan, E., & Rahmatullah, M. (2022). In Silico Prediction of Drug Metabolism and Toxicity Using ADMET Profiling Tools. *Journal of Applied Pharmaceutical Science*, *12*(4), 45–53. https://doi.org/10.7324/JAPS.2022.120406

Ferlay, J., Colombet, M., Soerjomataram, I., Parkin, D. M., Piñeros, M., Znaor, A., & Bray, F. (2021). Cancer Statistics for the Year 2020: An Overview. *International Journal of Cancer*, *149*(4), 778–789. https://doi.org/10.1002/ijc.33588

Globocan. (2020). Lung Fact Sheet. In *The Global Cancer Observatory* (Vol. 419).

Huang, H. J., Kraevaya, O. A., Voronov, I. I., Troshin, P. A., & Hsu, S. H. (2020). Fullerene derivatives as lung cancer cell inhibitors. *International Journal of Nanomedicine*, *15*, 2485–2499.

Huey, R., Morris, G. M., & Forli, S. (2012). *Using AutoDock 4 and AutoDock Vina with AutoDockTools: A Tutorial,*.

J, V., R, Z., L, J., J, M., P, S., V, P., MK, M., Z, L., J, L., C, G., N, S., I, Z., & DG, S. (2018). Mechanistic model-informed proarrhythmic risk assessment of drugs: review of the "CiPA" initiative and design of a prospective clinical validation study. *Clinical Pharmacology & Therapeutics*, *103*(1), 54–66. https://doi.org/10.1002/cpt.896

Jawarkar, R. D., Sharma, P., Jain, N., Gandhi, A., Mukerjee, N., Al-Mutairi, A. A., Zaki, M. E. A., Al-Hussain, S. A., Samad, A., Masand, V. H., Ghosh, A., & Bakal, R. L. (2022). QSAR, Molecular Docking, MD Simulation and MMGBSA Calculations Approaches to Recognize Concealed Pharmacophoric Features Requisite for the Optimization of ALK Tyrosine Kinase Inhibitors as Anticancer Leads. *Molecules*, *27*(15). https://doi.org/10.3390/molecules27154951

JB, H., & KE, K. (2008). Preclinical Pharmacokinetics in Drug Discovery: Structuring the Success Rate. *British Journal of Pharmacology*, *154*, 962–978. https://doi.org/10.1038/bjp.2008.157

Jung, Y. J., Lee, E. H., Lee, C. G., Rhee, K. J., Jung, W. S., Choi, Y., Pan, C. H., & Kang, K. (2017). AKR1B10-Inhibitory Selaginella Tamariscina Extract And Amentoflavone Decrease The Growth Of A549 Human Lung Cancer Cells In Vitro And In Vivo. *Journal of Ethnopharmacology*, *03*(010), 78–84. https://doi.org/10.1016/j.jep.2017.03.010

Kementerian Kesehatan Republik Indonesia. (2018). Pedoman Pengendalian Faktor Risiko Kanker Paru. In *Direktorat Jenderal Pencegahan dan Pengendalian Penyakit* (p. 29).

Kifle, Z. D., Tadele, M., Alemu, E., Gedamu, T., & Ayele, A. G. (2021). A recent development of new therapeutic agents and novel drug targets for cancer treatment. *SAGE Open Medicine*, *9*, 1–12. https://doi.org/10.1177/20503121211067083

Korrodi-Gregório, L., Soto-Cerrato, V., Vitorino, R., Fardilha, M., & Pérez-Tomás, R. (2016). From Proteomic Analysis To Potential Therapeutic Targets: Functional Profile Of Two Lung Cancer Cell Lines, A549 And SW900, Widely Studied In Pre-Clinical Research. *PLOS ONE*, *11*(11), 1–27. https://doi.org/10.1371/journal.pone.0165973

Kramer, J., & others. (2013). MICE models: Reducing risk of cardiac arrhythmias in drug development. *Journal of Pharmacological and Toxicological Methods*, *68*(1), 15–28. https://doi.org/10.1016/j.vascn.2013.04.001

Lazzarotto, M., Heinzen, V. E. F., & Yunes, R. A. (2005). Optimized modified Topliss method: A tool for quantitative structure-activity relationship studies. *Arzneimittel-Forschung/Drug Research*, *55*(10), 604–615. https://doi.org/10.1055/s-0031-1296911

Lin, J. J., Riely, G. J., & Shaw, A. T. (2017). Targeting ALK: Precision Medicine Takes on Drug Resistance. *Cancer Discovery*, *7*(2), 137–155. https://doi.org/10.1158/2159-

8290.CD-16-1123

Lynch, T., & Price, A. (2007). The effect of cytochrome P450 metabolism on drug response, interactions, and adverse effects. *American Family Physician*, *76*(3), 391–396.

Mody, H., Ramakrishnan, V., Chaar, M., Lezeau, J., Rump, A., Taha, K., Lesko, L., & Ait-Oudhia, S. (2020). A Review on Drug-Induced Nephrotoxicity: Pathophysiological Mechanisms, Drug Classes, Clinical Management, and Recent Advances in Mathematical Modeling and Simulation Approaches. *Clinical Pharmacology in Drug Development*, *9*(8), 896–909. https://doi.org/10.1002/cpdd.879

Morrissey, K., Yuraszeck, T., Li, C. C., Zhang, Y., & Kasichayanula, S. (2016). Immunotherapy and Novel Combinations in Oncology: Current Landscape, Challenges, and Opportunities. *Clinical and Translational Science*, *9*(2), 89–104. https://doi.org/10.1111/cts.12391

Muema, F. W., Liu, Y., Zhang, Y., Chen, G., & Guo, M. (2022). Flavonoids from Selaginella doederleinii Hieron and Their Antioxidant and Antiproliferative Activities. *Antioxidants*, *11*(1189), 1–16. https://doi.org/10.3390/antiox11061189

Nusantoro, D., & Fadlan, A. (2020). In Silico ADMET Profiling for Early Drug Discovery: Evaluating Pharmacokinetic and Toxicity Properties. *Jurnal Farmasi Sains Dan Komunitas*, *17*(2), 123–131. https://doi.org/10.24071/jpsc.2020.170201

Pardridge, W. M. (2012). Drug transport across the blood–brain barrier. *Journal of Cerebral Blood Flow and Metabolism*, *32*(11), 1959–1972. https://doi.org/10.1038/jcbfm.2012.126

Perazella, M. A., & Rosner, M. H. (2022). Drug-Induced Acute Kidney Injury. *Clinical Journal of the American Society of Nephrology*, *17*(8), 1220–1233. https://doi.org/10.2215/CJN.11290821

Pires, D. E. V, Blundell, T. L., & Ascher, D. B. (2015a). pkCSM: Predicting pharmacokinetic and toxicity properties. *Journal of Medicinal Chemistry*, *58*(9), 4066–4072.

Pires, D. E. V, Blundell, T. L., & Ascher, D. B. (2015b). pkCSM: Predicting small-molecule pharmacokinetic and toxicity properties using graph-based signatures. *Journal of Medicinal Chemistry*, *58*(9), 4066–4072. https://doi.org/10.1021/ACS.JMEDCHEM.5B00104/SUPPL_FILE/JM5B00104_SI_001.PDF

Puspita, R. (2018). Pemanfaatan Model Sel Caco-2 dalam Evaluasi Penyerapan Obat secara In Vitro. *Jurnal Farmasi Dan Ilmu Kefarmasian Indonesia*, *5*(2), 95–104.

Q, L., Y, H., & J, P. (2024). CrossFuse-XGBoost: accurate prediction of the maximum recommended daily dose through multi-feature fusion, cross-validation screening and extreme gradient boosting. *Briefings in Bioinformatics*, *25*(1), bbad511. https://doi.org/10.1093/bib/bbad511

Ren, M., Li, S., Gao, Q., Qiao, L., Cao, Q., Yang, Z., Chen, C., Jiang, Y., Wang, G., & Fu, S. (2023). Advances in the Anti-Tumor Activity of Biflavonoids in Selaginella. *International Journal of Molecular Sciences*, *24*(9), 1–24. https://doi.org/10.3390/ijms24097731

RJ, A., GP, A., ES, B., N, K., GA, K.-U., D, L., TH, K., & for the Study of the Liver, E. A. (2019). EASL Clinical Practice Guidelines: Drug-induced liver injury. *J Hepatol*, *70*(6), 1222–

1261. https://doi.org/10.1016/j.jhep.2019.02.014

Sanguinetti, M. C., & Tristani-Firouzi, M. (2006). hERG potassium channels and cardiac arrhythmia. *Nature*, *440*(7083), 463–469. https://doi.org/10.1038/nature04710

Sari, I. W., Junaidin, J., & Pratiwi, D. (2020). STUDI MOLECULAR DOCKING SENYAWA FLAVONOID HERBA KUMIS KUCING (Orthosiphon stamineus B.) PADA RESEPTOR α-GLUKOSIDASE SEBAGAI ANTIDIABETES TIPE 2. *Jurnal Farmagazine*, *7*(2), 54. https://doi.org/10.47653/farm.v7i2.194

Serafini, M. M., & others. (2024). Recent advances and current challenges of new approach methodologies for adult and developmental neurotoxicity assessment. *Archives of Toxicology*, *98*, 123–145. https://doi.org/10.1007/s00204-024-03703-8

Siswandono. (2016). *KIMIA MEDISINAL 1* (2nd ed.). Airlangga University Press.

Siswandono & Soekardjo, B. (2017). *Kimia Medisinal* (Edisi 2). Airlangga University Press.

Smith, D. A., Di, L., & Kerns, E. H. (2018). The effect of plasma protein binding on in vivo efficacy: misconceptions in drug discovery. *Nature Reviews Drug Discovery*, *17*(10), 697–707. https://doi.org/10.1038/nrd.2018.134

StatPearls. (2024a). *Drug Clearance*. StatPearls Publishing.

StatPearls. (2024b). *Pharmacokinetics*. StatPearls Publishing.

T, C., B, F., G, G., JB, P., P, S., Y, S., DG, S., & N, S. (2016). The Comprehensive in Vitro Proarrhythmia Assay (CiPA) initiative — Update on progress. *Journal of Pharmacological and Toxicological Methods*, *81*, 15–20. https://doi.org/10.1016/j.vascn.2016.06.002

T, H., D, D., & S, B. (2023). Drug-induced liver injury: a comprehensive review. *Ther Adv Gastroenterol*, *16*, 17562848231163410. https://doi.org/10.1177/17562848231163410

Tejera, E., Munteanu, C. R., López-Cortés, A., Cabrera-Andrade, A., & Pérez-Castillo, Y. (2020). Drugs Repurposing Using QSAR, Docking and Molecular Dynamics for Possible Inhibitors of the SARS-CoV-2 Mpro Protease. *Molecules (Basel, Switzerland)*, *25*(21), 5172. https://doi.org/10.3390/molecules25215172

WCRF. (2022). *Worldwide Cancer Data*. World Cancer Research Fund.

Zanger, U. M., & Schwab, M. (2013). Cytochrome P450 enzymes in drug metabolism: Regulation of gene expression, enzyme activities, and impact of genetic variation. *Pharmacology \& Therapeutics*, *138*(1), 103–141. https://doi.org/10.1016/j.pharmthera.2012.12.007

Zou, Z., Kang, F., Zhang, S., Chen, D., Tan, J., Kuang, M., Zhang, J., Zeng, G., Xu, K., & Tan, G. (2021). Biflavonoids from Selaginella doederleinii as Potential Antitumor Agents for Intervention of Non-Small Cell Lung Cancer. *Molecules*, *26*(5401), 1–13.